

## RESEARCH ON THE APPLICATION OF PILE-BUCKET COMPOSITE STRUCTURE IN THE SILT COAST

*Yao Liu<sup>1,2</sup>, Jintian Chen<sup>3</sup> and Wu Li<sup>4\*</sup>*

1. *College of Civil Engineering, Northeast Forestry University, Harbin 150040, China; dltmly@nefu.edu.cn*
2. *College of Engineering, Department of architectural Engineering, Kangwon National University, Chuncheon-si, 24341, Republic of Korea*
3. *College of Civil and Architectural Engineering, Heilongjiang Institute of Technology, Harbin 150050, China; cccjt2003@163.com*
4. *CCCC Third Harbor Consultants Co., Ltd, Shanghai 200023, China; liw@theidi.com*

### ABSTRACT

With the over-exploitation of high-quality coastlines, the site selection and construction of new ports have to be expanded to silt coast, which will bring about quite many technical difficulties in the construction of wharves and revetments, and the cost of investment will also rise sharply. In this paper, a kind of combined design scheme of the high-pile wharf and the bucket structure is proposed to solve the problems mentioned above. The high-pile wharf structure is meant to adapt to the silt foundation, while the bucket can help to improve the ground bearing capacity. The stability and displacement of the bucket structure, and the influence of displacement on high-pile wharf during the service period are analyzed using a finite element model. Analysis results indicate that the horizontal and vertical displacements of the bucket structure in the service period are reduced to same extent compared with those in the construction period, and the maximum horizontal displacements of the lower barrel structure are 0.4cm more than those of the upper part. The difference between the vertical displacement on the seaside and the portside is 10.5cm, and a rotation of 0.2° occurred in the bucket. Besides, the working loads above the bucket have a significant influence on the horizontal displacement and sliding stability of the bucket in the service period. It can be known from the above conclusion that the composite structure is a kind of structure that can adapt to the conditions of soft soil underwater, and it has advantages of the construction period and cost when used in water depth and silt area, which provides useful experience for the silt coastal projects.

### KEYWORDS

Pile-bucket combination, Silt coast, Stability, Displacement analysis

### INTRODUCTION

In order to meet the demands of economy, society and environment, the scale of ports is constantly expanded, and large-scale, deep-water, specialized and multifunctional wharfs have become a trend of port development. However, many ports are faced with problems such as limited function and overloading operations, the conflict between the development of ports and cities, environmental issues, and unmatched modes of transport, which need to be further improved. To ease the tensions mentioned above, new ports have to be built in seas where the hydrogeological conditions are very complicated, thus greatly increases the technical difficulty of wharf, revetment and other projects. Silty coastal zones are widely distributed around the world, Holland in western Europe, Bohai Bay in China and the south-central coast of Jiangsu are the most famous silty coasts

in the world. 4000km of the 18000km continental coastlines are silty [1-3]. The critical technical difficulties in those areas are mainly concerned with the treatment of thick weak soil stratum and the improvement of its high sensitivity and poor mechanics properties. As shown in figure1-3, the traditional way of drainage consolidation, layered filling of sand, and mud replacement by blasting are defective in that the amount of engineering is tremendous, the duration of the project is long, the influence on the environment is great, and the process is easily interrupted by gales. In particular, mud replacement by blasting will make a severe impact on the marine environment, a large number of sea creatures will be killed during the construction [4,5].



*Fig.1- A drainage plate*



*Fig.2 - Filling sand*



*Fig.3 - Blasting compaction*

The development of main technologies of bucket foundation can be traced back to the 1960s. Since Statoil successfully applied bucket foundation platform at sea for the first time in 1994, the research and application of bucket foundation platform has been gradually popularized all over the world [6]. The use and research of bucket foundation started relatively late in China. Bucket foundation structure is a new type of structure suitable for offshore soft soil foundation. At present, scholars at home and abroad have carried out relevant research on bucket infrastructure [7,8]. Liu et al. studied the horizontal limit bearing capacity of bucket foundations and the distribution of the active and passive earth pressure by means of model tests and finite element method. The formula for evaluating the horizontal limit bearing capacity is suggested, and the horizontal bearing capacity of double buckets foundation is investigated and a means to estimate the bearing capacity of the double buckets foundations is given [9]. Cai et al. studied the numerical analysis of earth pressure, anti-overturning calculation, and numerical simulation during construction and operation period of bucket foundation structure, which provides a theoretical basis for the design and construction of large cylinder structure [10-12]. Cao et al. analyzed of the soil pressure and the barrel's vertical and circular distributions are performed with different thickness of reclamation silt, which provides a reference for checking the stability of new bucket foundation revetment structure [13]. Byrne et al. based on the experimental results, an incisive understanding of the relationship between load and displacement is obtained, and a simple theoretical and numerical model is proposed [14]. Park et al. established the finite element model of bucket foundation on sandy soil foundation and layered foundation, and studied the characteristics of vertical bearing capacity. The results show that the shear strength of sand and clay will affect the shape of failure surface of bucket foundation [15,16].

The traditional gravity wharf has high requirements for foundation. In the deep-sea area with thick, soft soil layer, it needs a lot of foundation treatment. The project investment is large and the construction period is long. It is unreasonable from the economic and technical considerations. As one of the main structural types of port terminals, high pile wharf is widely used because of its light structure, adaptability to soft soil foundation and little impact on water flow. little influence on water flow [17]. It is widely used in China's coastal and inland rivers and other soft soil foundations, such as the Yangtze River Delta region, Pearl River Delta region, Lianyungang, Tianjin and other areas, where there is a deep silt layer, especially suitable for deep foundation structures such as high pile wharf. In order to adapt to the complex characteristics of various foundations, which has experienced different forms of development and derived many new structural types.

In this paper, a new type of structure pile-bucket wharf is proposed, shown in Figure 4. The configuration is of great practical use in that it helps to save much effort from the treatment of soft soil, which is substituted by the soil concealing by cover plate, wallboards, septums, and the hard





(b) *Plan view of bucket structure*

*Fig.5 - Schematic diagram of bucket structure*

## COMPUTING MODEL AND PARAMETERS

### Numerical model calculation assumptions

The numerical analysis software used is PLAXIS, and the 2D plane finite element method is used for the theoretical analysis. Bucket structure runs longer in vertical direction. According to the characteristics of the structure and deformation, such structure should have the properties of plane strain. To ensure the accurate reflection of its properties, the plane strain model is used in this paper to simulate the bucket structure, not only can reflect the essence of the problem, but also can save a lot of calculation time. The constitutive relationship of soil often plays a decisive role in the calculation results, so the Mohr-Coulomb Model is used for calculation [18]. According to the characteristics of the project and geological reports, several typical soils in different strata are selected as samples. In the period of construction and service, the fluid-solid interaction has been considered in the computing model. The dewatering boundary status is set as the left side, and the upside of the model is to drain, while the right side and the bottom are not to drain.

As shown in Figure 5, because of the medial septum, the structure has a strong metope connection that enhances the flexural rigidity, so it must be considered in computing. The upper wall, the lower wall, sidewall, and inner septum of the bucket are simulated in plate units. Considering the support served by the lower wall of the bucket in the longitude direction, it is simulated in the horizontal plate unit model, in which the longitudinal compressional stiffness of the coverage area is adopted as the rigidity. The status of material is supposed as elastic. The inner configuration is set as actual, and the fillings are taken as corresponding soil or rocks.

### Numerical model meshing

In the simulating process, the properties of the soil, the composite soil for strengthening the sand piles, the backfill sand, the riprap, and the dredger soil are taken as the Mohr-Coulomb elastic-plastic model. The piles of the wharves are simulated in pile units. The caps, the roads, the surface layer of the yard, the upper bucket wall, the top cover, and the inner septum of the lower bucket are simulated in isotropic elastic plate units [20]. In order to simulate the interaction and how loads are transferred between the structure and the ground, the surface of the structure is simulated in interface units, whose parameters are set as those of the adjacent stratum. According to the basic requirements and structural characteristics of the numerical simulation, the range of the numerical simulation soil is 5 times the horizontal dimension of the structure on each side in the horizontal direction, 2 times the depth of the structure in the depth direction, and the boundary of the soil is fixed.

Based on the characteristics of the project and previous experience, the calculating area is determined as: in the horizontal direction. The portside and seaside boundary are set as 65 meters and 55 meters separately away from the axle wire of the bucket's foundation; in the depth direction, the upside and bottom boundary are set as 50 meters and 8 meters separately away from the sea level [21]. The numerical calculation model is shown in Figure 6, and how the mesh is divided is illustrated in Figure 7.

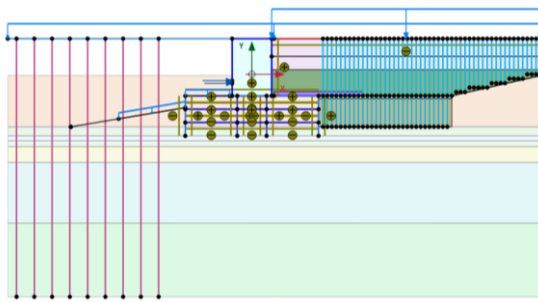


Fig.6 - Finite element analytical model

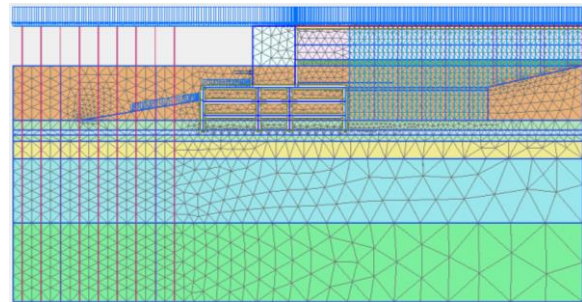


Fig.7 - Mesh model of bucket's foundation

### Parameter selection of soil and engineering structure related material

The parameters in the numerical model are mainly concerned with the physical and mechanical properties of the soil, the composite soil for strengthening the sand piles, the reclaimed silt, the sandbags, the riprap, the piles and caps of the wharf, the surface layer of the yard, the walls of the upper part of the bucket, the top cover of the lower part of the bucket, the inner septum and the inner walls of the lower part of the bucket [22].

#### Physical and mechanical parameters of soil

The calculation parameters are selected according to the report of engineering geological exploration, including: bulk density of soil, elastic modulus  $E$ , Poisson's ratio  $\mu$ , cohesion  $c'$ , internal friction angle  $\phi'$ , permeability coefficient  $k$ . According to the geological data, the detailed selection of the main physical and mechanical parameters of the soil on both sides of the structure is shown in Table 1. The values of  $c'$  and  $\phi'$  are the rapid shear strength of consolidation. The drainage type used for silt and silty clay is no-drainage, and that of sandy silt and silty sand is drainage.

Tab.1: Physical and mechanics properties of the soil

Stratum name	Moisture content $w$ (%)	Natural weight-specified density $\gamma$ kN/m <sup>3</sup>	Initial void ration $e_0$	Poisson ration $\mu$	Compression modulus $E_s$ (MPa)	Compression coefficient $a$ (MPa <sup>-1</sup> )	Strength parameters	
							Cohesion $c'$ (kPa)	Internal friction angle $\phi'$ (°)
Silt	69.7	15.8	1.963	0.42	1.4	2.17	8.5	8
Silty clay	28.4	19.7	0.807	0.42	5.8	0.31	35	15
Sandy silt	25.1	19.8	0.701	0.40	11.1	0.16	4.5	31.5
Silty sand	22.9	20.0	0.649	0.40	13.8	0.12	1.5	38

#### Physical and mechanical parameters of reclaimed silt

Layered backfilling is adopted for the backfilling behind the bucket. Considering that the compactness of the lower reclaimed silt increases under the action of the upper reclaimed silt, in order to more reasonably simulate the characteristics of the reclaimed silt, the reclaimed silt is divided into the upper layer (0-7m in depth) and the lower layer (7m in depth to the excavation face), and the corresponding calculation parameters are adopted. The drainage type adopted for reclaimed silt is no-drainage. The physical and mechanical parameters are shown in Table 2.

Tab 2: Physical and mechanics properties of the reclaimed silt

Stratum	Natural weight-specified density $\gamma$ (kN/m <sup>3</sup> )	Initial void ration $e_0$	Poisson ration $\mu$	Compression modulus $E_s$ (MPa)	Strength parameters (service period)		Strength parameters (construction period)	
					$c'$ (kPa)	$\phi'$ (°)	$c'$ (kPa)	$\phi'$ (°)
Reclaimed silt (0-7m in depth)	14	1.4	0.42	2	15	0.6	5	0.6
Reclaimed silt (7m in depth to the excavation face)	14	1.4	0.42	2	15	0.6	9	0.6

### **Physical and mechanical parameters of soil reinforced by sand pile**

The depth range of about 10m behind the bucket body is mainly silty soil. In order to ensure the stability of the reclaimed silt, sand piles are needed to reinforce the soil layer below. The vertical drainage lines are arranged at an interval of 1m within the area of sand pile reinforcement to simulate the vertical drainage effect of sand piles. At the same time, the sand cushion is above the sand pile reinforcement area. The sand pile reinforcement scheme for ramp wharf, the diameter of sand pile is 1m. In order to facilitate finite element analysis and calculation by conventional stability analysis program, the values of  $c$  and  $\phi$  needs to be expressed by equivalent strength. That is, the Priebe method is used. The equivalent physical and mechanical parameters of composite foundation reinforced by sand pile are shown in Table 3.

*Tab.3: Mechanics properties of the composite soil reinforced by sand piles*

Stratum	Displacement ratio of sand piles	Natural weight-specified density $\gamma$ (kN/m <sup>3</sup> )	Initial void ration $e_0$	Poisson ration $\mu$	Compression modulus $E_s$ (MPa)	Strength parameters	
						Cohesion $c_{sp}$ (kPa)	Internal friction angle $\phi_{sp}$ (°)
Composite soil reinforced by sand piles	30%	16.6	0.5	0.40	3.12	12.69	15.44

Note:  $E_s$  = compression modulus of sand pile composite foundation;  $c_{sp}$  = cohesion of composite foundation;  $\phi_{sp}$  = internal friction Angle of composite foundation.

### **Physical and mechanical parameters of riprap bedding and backfill sand in upper bucket**

The bottom protection at the seaside is filled with 200~400kg block stones with a thickness of about 2m, and the filling range is 25m outside the bucket; the bottom protection at the portside is filled with 200~400kg block stones with a thickness of about 1m, and the filling range is 20m outside the bucket. The riprap on the seaside can be simulated in the form of uniform load, and the solid element simulation is applied to the riprap on the portside because of the need of backfilling silt and the reinforcement of the foundation. The bucket foundation is a gravity structure and the gravity of the backfill sand in the upper bucket is the resistance to prevent the bucket structure from slipping or overturning. The physical and mechanical parameters of riprap bedding and backfill sand are shown in Table 4.

*Tab.4: Mechanics properties of the riprap bedding and the backfill sand of the bucket's upper part*

Stratum	Weight-specified density $\gamma$ (kN/m <sup>3</sup> )	Poisson ration $\mu$	Elasticity modulus $E$ (MPa)	Cohesion $c'$ (kPa)	Internal friction angle $\phi'$ (°)
Riprap bedding	10	0.3	20	0	45

---

Backfill sand	18	0.3	20	0	28
---------------	----	-----	----	---	----

---

***Mechanical parameters of bucket structure***

Considering the structural form and stiffness characteristics of the barrel body, the compression and flexural stiffness of each part of the bucket body are converted respectively according to the principle of equivalent stiffness, and the unit weight of each part of the bucket structure is calculated according to the principle of equal weight. In the finite element model, the semi-circular parts at both ends of the lower bucket walls are simulated by the vertical plate elements, the vertical plate element is also used to simulate the vertical septum in the short axis direction inside the bucket. The outer bucket wall in the long axis direction of the foundation bucket and the internal vertical septum have the function of supporting the bucket in the horizontal direction, and are simulated by the horizontal plate element, its mechanical parameters are converted according to the equivalent flexural stiffness in the horizontal direction. The walls of the bucket's upper part are simulated by vertical plate element, the top cover of the bucket's lower part is simulated by horizontal plate element. The corresponding mechanical parameters of each part of the bucket structure are shown in Table 5.

*Tab. 5: Mechanics properties of the bucket*

Locations of structure	Compressive stiffness EA (kN/m)	Bending stiffness EI (kN·m)	Weight-specified density W (kN/m <sup>2</sup> )	Poisson ration $\mu$
Walls of the bucket's upper part	1.72E7	4.00E5	12.72	0.2
Inner cross septum of the bucket's lower part	9.70E6	7.30E6	4.5	0.2
Inner vertical septum of the bucket's lower part	2.93E7	1.97E6	7.2	0.2
Walls of the bucket's lower part	1.95E7	5.84E5	14.40	0.2
Top cover of the bucket's lower part	1.30E7	1.73E5	9.60	0.2

***Mechanical parameters of wharf high pile, wharf roof and wharf yard***

Wharf high piles are precast concrete pipe piles, which are simulated by embedded pile element. Plate element is used to simulate wharf roof and yard. The corresponding mechanical parameters are shown in Table 6 and Table 7 respectively.

*Tab.6: Properties of the wharf's high-piles*

Type of piles	E (kN/m <sup>2</sup> )	$\nu$ (kN/m <sup>3</sup> )	D (m)	Thickness (m)	Distance between piles Lspacing (m)
Precast circular pipe pile	3.6E7	24.00	1.2	0.145	4

*Tab.7: Properties of the wharf's roof and yard*

Structural part	Compressive rigidity EA (kN/m)	Bending rigidity EI (kN·m)	Weight-specified density W (kN/m <sup>2</sup> )
Wharf roof	7.65E7	4.15E7	61.20
wharf yard	1.50E7	3.10E5	12.00

## NUMERICAL SIMULATION ANALYSIS AND DISCUSSION

Considering the drainage consolidation effect of the soil during the service period, the consolidation time of the soil is taken as 5 years in order to achieve full drainage. For the sake of simplicity, the service life mentioned later, if not indicated, is calculated after 5 years.

### Excess pore water pressure during the service period

In order to analyze the excess pore water pressure during the service period, four sample points are selected, namely A (30, 4), B (30, 1.749), C (30, -12.743), D (30, -25.795), based on which the curve of the excess pore pressure in the construction period and service period (5 years in total) is depicted, shown in Figure 8. The first and second points are selected from the reclaimed silt, the 3rd point is selected in the lower part of the silty clay, and the 4th point is selected from the stratum of silty sand. The construction period is terminated in the 20th month [18,22].

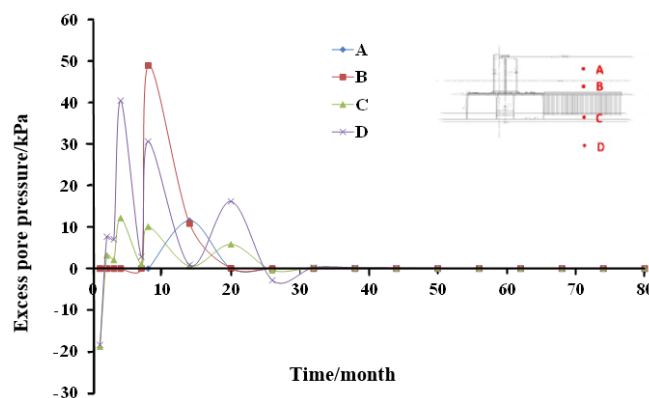


Fig.8 - Excess pore pressure curve of sample points in soil

It can be known from Figure 8 that in the construction period, the excess pore pressure firstly rises rapidly as a consequence of the preloading and the increased pressure caused by reclaimed silt, whereas it has shown a decline after the reclaimed silt is air-cured and the soil is drained and consolidated. In the service period, the excess pore pressure in reclaimed silt decreases with the removal of the preloading. In the next stage, it goes up with the imposing of loads in the service period. At last, the excess pore pressure dissipates. What's more, both curves almost overlap with each other, and the values are relatively close. By the end of the first year, the value of excess pore pressure is close to 0. The excess pore pressure in the lower part of the sand piles and the stratum of silty sand firstly goes down and then goes up in the first year. Afterward, it slowly decreases, and by the fifth year, the value is close to 0. With the installation of the drainage pipes, the shallower the stratum is, the more rapid the excess pore pressure dissipates. From the conclusions drawn above, we can see that it is reasonable to set the simulation duration as 5 years for the working condition in the service period, for by this time, the structure and the displacement of soil is relatively stable, and the results can be identified as the final values.

### Horizontal displacement during the service period

At the condition of extremely low water level during the service period, after the sand piles and the foundation of reclaimed silt are reinforced, there is a working load of 3t to 5t distributed on the structure. In the calculating, a uniform load of 50kPa is used. The extremely low water rests at -0.68m, whose recurrence interval is 50 years [18,23-25]. The nephogram of the horizontal displacement during the service period is demonstrated in Figure 9.

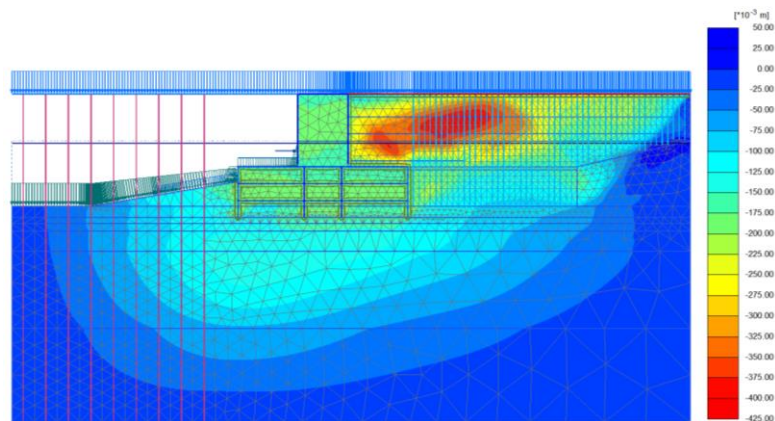


Fig.9 - Horizontal displacement nephogram in-service period

The horizontal displacement distribution along the direction of depth of the upper part of the bucket is illustrated in Figure 10, and how the maximum horizontal displacement of the upper part of the bucket changes over time during the construction and service period is shown in Figure 11. The figures show that the maximum horizontal displacement of the upper part of the bucket roughly follows the distribution of the parabola. At the beginning of the service period, with the withdraw of the preload (10t) and the exerting of comparatively small loads (5t), the horizontal displacement of the bucket decreases rapidly because of the unloading and resilience, whose reduction weights at 2cm. As time goes on, the horizontal displacement shows a minor decline and tends to be stable afterward. The total spring back in 5 years is about 0.4cm. After the fifth year, the maximum final horizontal displacement appears at the elevation of +2.11m, which is measured as 18.8cm. According to the numerical calculation results, the horizontal displacement of the barrel is 20cm in the silt foundation, which has little influence on the soil deformation beyond 200cm and can be neglected. In addition, the straight pile foundation has a certain ability to resist horizontal pressure, the strength index of the silt foundation is low, so the soil deformation can be dissipated around the pile foundation.

The region of the moving soil mass extends below the wharf structure, which affects the three rows of piles on the land side of the wharf, the bending moment on the pile shaft increases, but it is within the bearing range of the pile foundation. Therefore, it is suggested that the batter piles are arranged in the front of the wharf and stay away from the area of moving soil mass, so that the stresses caused by it can be decreased.

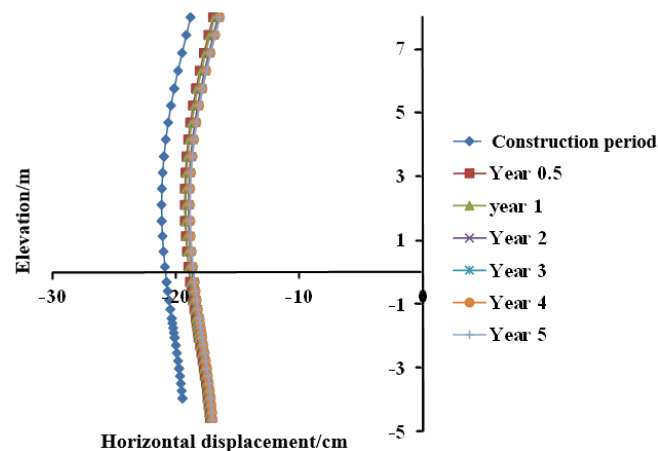


Fig.10-Distribution of horizontal displacement in the depth direction of upper part of the bucket

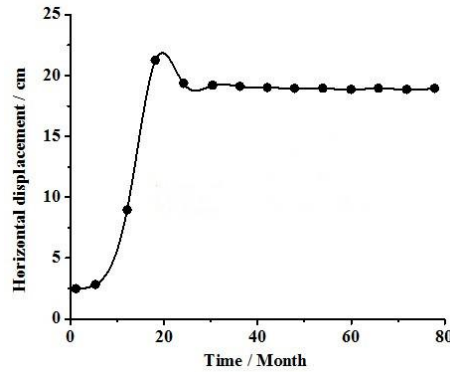


Fig.11-The maximum horizontal displacement of the upper part of the bucket

The horizontal displacement distribution along the direction of depth of the lower part of the bucket is illustrated in Figure 12, and how the maximum horizontal displacement of the lower part of the bucket changes over time during the construction and service period is shown in Figure 13. The figure shows that the horizontal displacement in the direction of depth in the service period roughly increases with depth, except for some abrupt breaks at the interfaces. At the beginning of the service period, with the withdraw of the preload (10t) and the exerting of comparatively small loads (5t), the horizontal displacement of the bucket decreases rapidly because of the unloading and resilience, whose reduction weights at 3cm. As time goes on, the variation trend of horizontal displacement over time is almost the same as that of the upper bucket. The total spring back in 5 ars is about 0.2cm. After the fifth year, the final maximum horizontal displacement happens at -13.85m, measured as 19.2cm [22,26].

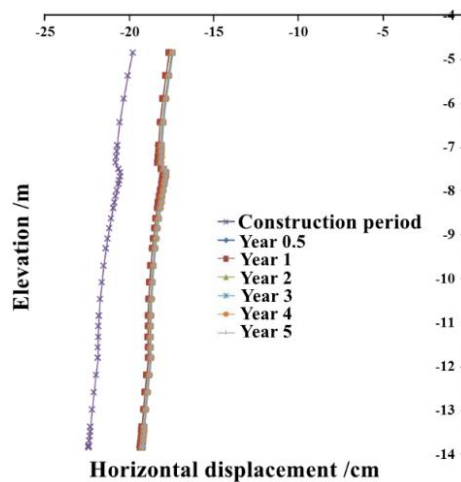


Fig.12-Distribution of horizontal displacement in the depth direction of lower part of the bucket

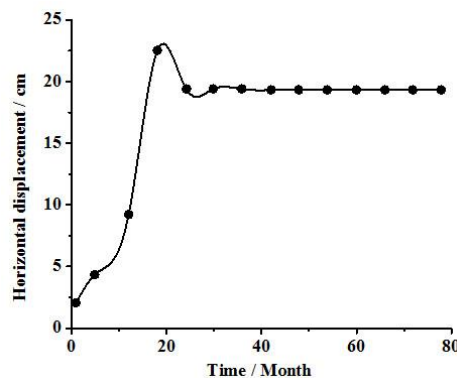


Fig.13-The maximum horizontal displacement of the lower part of the bucket

After the completion of the construction of bucket foundation structure and backfilling silt behind it, a 50kPa load is applied above the structure and backfilling silt to represent the vehicle load during the service life. Under the action of this service load, the instantaneous excess pore water pressure is generated in the silt and acts on the bucket wall on the portside. At this time, the effective stress of the soil has not yet played a role, the lateral pressure coefficient is close to the water pressure state of 1.0. Therefore, the bucket body will have a large horizontal displacement increment at the beginning of service period (the first year). With the development of time, the excess pore water pressure in soil dissipates continuously, the force acting on the barrel wall gradually transformed into the synergy of effective soil pressure and water pressure, the lateral pressure coefficient of soil is smaller than that of water, so the value of horizontal pressure in the later service period will be lower than that in the early service period. Hence, the bucket body has a certain rebound, the horizontal displacement decreases, but not much reduction in total.

Therefore, it is suggested that the ground treatment behind the bucket structure should be started as early as possible, making sure that the soil deformation is completed within the duration of foundation construction. Then proceeds with the front wharf construction, which can effectively reduce the soil deformation caused by the load during the service life.

### Analysis of slippage of the structure in the service period

The vertical displacement of the top cover of the bucket's lower part along the long axis during the service period (5years) is shown in Figure 14, the maximum vertical displacement will reach 31.6cm, and the variation trend of slip angle of the bucket over time is shown in Figure 15. The figures show that the vertical displacement of the top cover of the lower part of the bucket keeps on increasing from the seaside to the portside in the service period. In the construction period and service period, the vertical displacement on the portside in both conditions is almost the same. However, the vertical displacement on the seaside in the service period shows an increase compared with that in the construction period, and the rotation angle decreases to a certain extent. The vertical displacement on the portside and seaside is 31.6cm and 21.1cm respectively, it can be seen that the differential settlement is quite large. Considering the length of bucket's lower part in axial direction (30m), a rotation of  $0.2^\circ$  occurred in the bucket. Therefore, it is possible to slip [27].

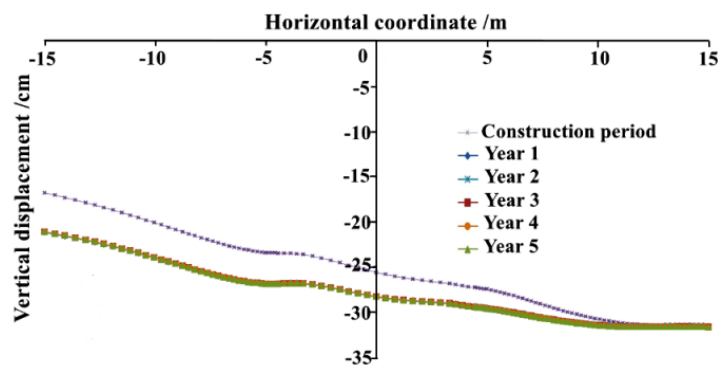


Fig.14-Distribution of vertical displacement along the horizontal direction of the top cover of bucket's lower part in-service period

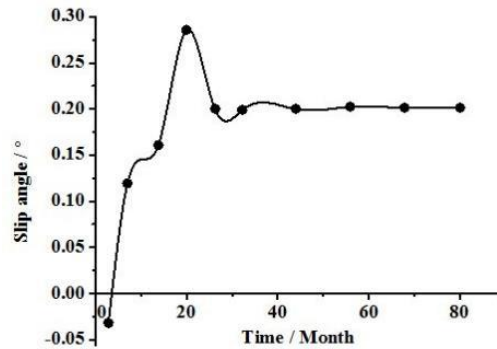
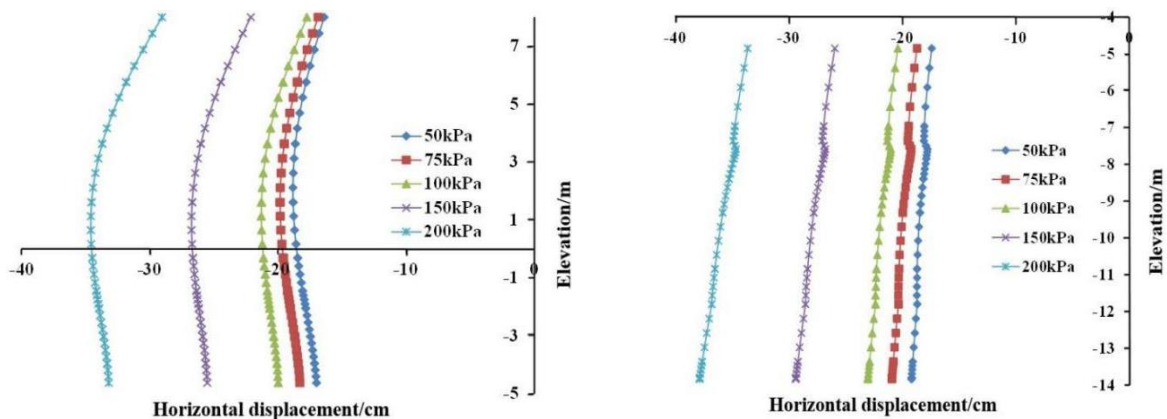


Fig.15-Changing curve of slip angle of the bucket

### Stability analysis of the bucket under different working loads

The working load in the previous calculating is 50kPa, which is uniformly distributed over the structure and the backfilled silt. In this paper, the stability analysis is made under different working loads in service periods. In this paper, an exploratory analysis is made on the stability of the bucket under different working loads. It can be seen from Figure 16 to Figure 18 that the sliding angle of the bucket and the maximum displacement of both the upper part and the lower part of the bucket are concerned with working loads. The sliding angle of the bucket increases approximately linearly with working loads. The maximum horizontal displacement of the upper part and the lower part of the bucket grows with working loads, which shows a tendency to accelerate [28,29].



(a) Horizontal displacement of upper bucket (b) Horizontal displacement of lower bucket

Fig.16 - Horizontal displacement of the bucket under different working loads in service period

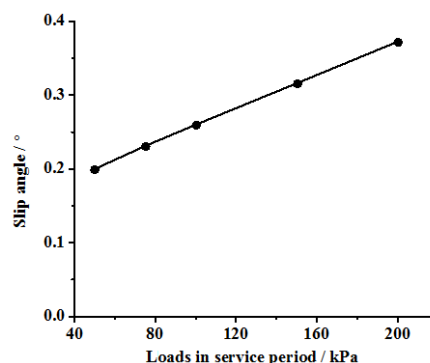


Fig.17 - Sliding angle of the bucket under different working loads in service period

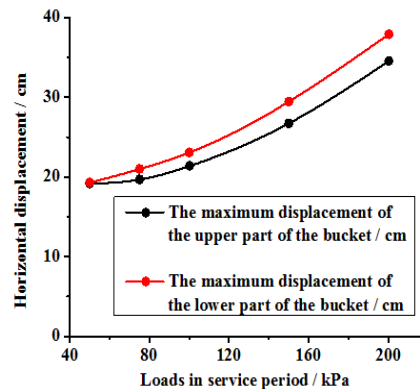


Fig.18 -The maximum horizontal displacement of the bucket under different working loads in service period

The working loads applied from above have an obvious influence on the horizontal displacement and the sliding stability of the bucket. The working loads in service period should be controlled properly according to the actual deflection indexes. In this way, the sliding of the structure caused by excess horizontal displacement and uniform settlement, which results from long-term overloading, can be avoided.

### Distribution of plastic zones in soil mass during the service period

The distribution of soil plastic zone in the first and fifth years is shown in Figure 19. Figure 20 illustrates the distribution of shearing stress of the soil mass (1m below the end of the lower bucket) in service period. As can be seen from the figures below, the distribution of plastic zone in the soil during the service period does not expand significantly, it is mainly distributed in the soil below the bucket and the natural silt at the right side of the reinforced area by sand pile, without connecting with each other to form a sliding surface, and the shearing stress in the soil below the bucket is lower than the shearing strength [19, 30]. The average utilization rate of shearing strength is distributed between 0.4 and 0.9.

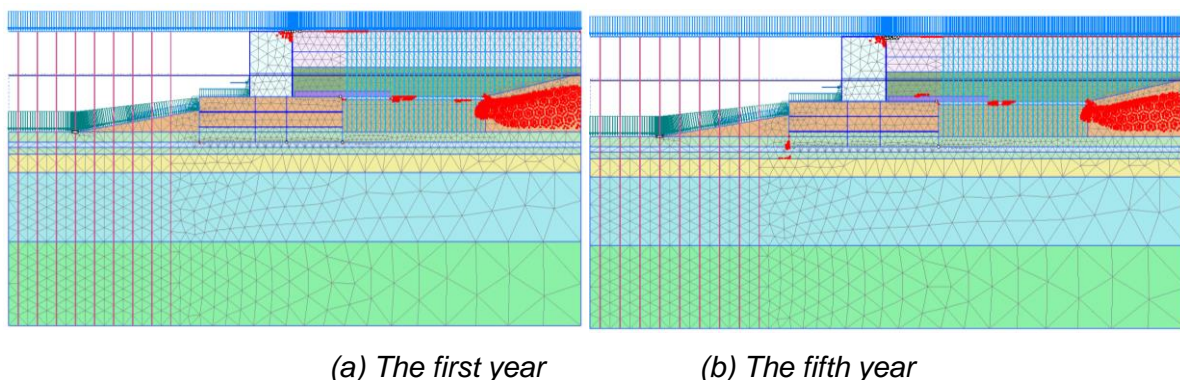
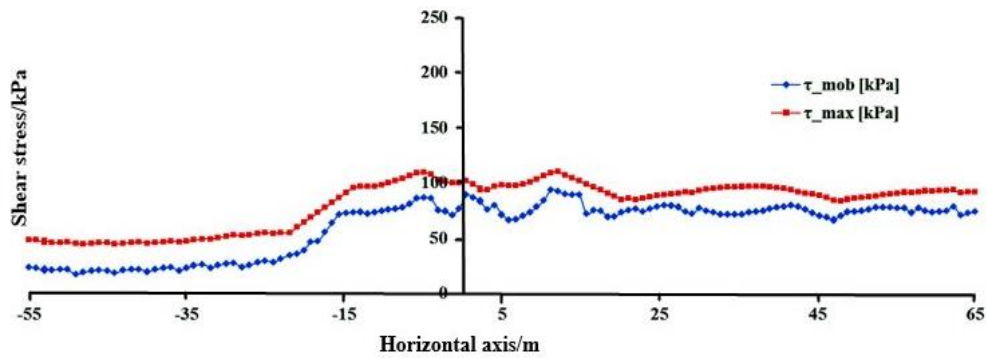
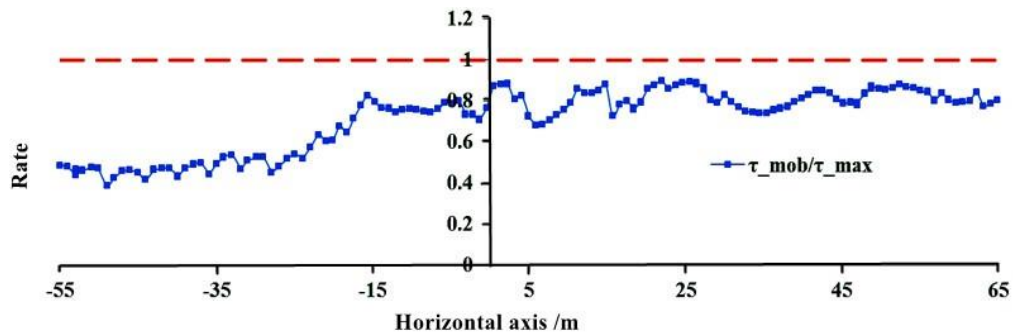


Fig.19 - Distribution of plastic zones in soil mass in service period



(a) Comparison of shearing stress  $\tau_{mob}$  and shearing strength  $\tau_{max}$  of the soil mass



(b) Utilization rate of shearing strength of soil mass  $\beta = \tau_{mob}/\tau_{max}$

Fig.20 - Distribution of shearing stress of the soil mass below the bucket

## CONCLUSION

The new bucket-based structure is proposed according to actual project in this study, the research results are mainly to solve application problems in engineering. Based on the numerical simulation and analysis of the interaction between bucket and soil during the service period, the conclusions can be drawn as below:

- (1) During the service period, the horizontal displacement and vertical displacement of the bucket structure have a certain change comparing with the construction period, that is, various displacements decrease due to the rebound effect of the load reduction. However, the deformation tends to be stable due to the drainage consolidation effect of preloading, so the change is small. After 5 years of drainage consolidation, the maximum horizontal displacement of the upper bucket structure is 18.8cm and the horizontal displacement of the lower part reaches 19.2cm.
- (2) The slippage degree of bucket structure is reduced compared with the construction period. The maximum vertical displacement of the bucket is 31.6cm in the service period, which occurs on the port side. The difference of the vertical displacement between the seaside and the portside of the bucket is 10.5cm, and the bucket rotates  $0.2^\circ$ , which is  $0.08^\circ$  less than that of the construction period.
- (3) The working loads from above bucket have a significant influence on the horizontal displacement and sliding stability of the bucket in the service period. The slip Angle of the bucket increases with the increase of the working load linearly. The maximum horizontal displacement of the upper and lower bucket also increases and has a trend of accelerating increase. Therefore, it is suggested that the working loads in the service period should be controlled strictly according to the actual deformation control index of the bucket to avoid excessive horizontal displacement caused by long-term overload and structural sliding caused by uneven settlement.
- (4) In the stable phase of the service period, the plastic zone of the soil in the lower part of the bucket does not form a through plastic shear zone, the shearing strength of the soil has not been fully utilized. The average utilization rate of the shear strength is distributed between 0.4-0.9, and the overall stability of the bucket foundation will not be damaged.
- (5) It is recommended that the wharf's construction go after that of the bucket and the ground treatment behind the bucket, for it will help reduce the impact of the deflection of the soil caused by the bucket on the foundation of the wharf. Besides, it is best that the batter piles are furnished in the front of the wharf to stay away from the area of moving soil mass, for it helps to reduce the stresses caused by it.
- (6) According to the actual monitoring data of the barrel structure, the displacement of the barrel is smaller than the result of the numerical calculation, the displacement trend is consistent, and the displacement is on the same order of magnitude. For the actual project, this error is within the allowable range of the project.

## ACKNOWLEDGEMENTS

This research was funded by the Fundamental Research Funds of the Central Universities, grant number 2572018BJ15, and the Science and Technology Project of the Department of Transportation of Heilongjiang Province, grant number 2021HLJ01K42.

## REFERENCES

- [1] Wang, Y.Q. Some understandings in soft soil improvement in Tianjin Port. China Harbour Engineering 2006, 1, 6-19.
- [2] Ding, J.H.; S.X.; G.Z. Theory and practice of deep waterway on silt coast in LianYungang (Preliminary basics). China Communications Press: Beijing, China, 2012.
- [3] Wang, Y. Coastal and Marine sciences. Beijing: Science Press, 2016.
- [4] Baerheim, M.; Hoberg, L.; Tjelta, T. I. Development and structural design of the bucket foundations for the Europe jacket. Offshore Technology Conference, Houston, Texas, 1-4 May, 1995.

- [5] Yu, Y.H.; T, S.L. Method of quick construction of wharf on weak soil. *Journal of Ocean Technology* 2006, 25, 122-126.
- [6] Bye, A.; Erbrich, C.; Tjelta, T.I. Geotechnical design of bucket Foundations. *TC7793, OTC'27*, 1995, 869-883.
- [7] Zhang, S.H.; Zheng, Q. A.; Liu, X. N. Finite element analysis of suction penetration seepage field of bucket foundation platform with application to offshore oil field development. *Ocean Engineering* 2004, 31(11): 1591-1599.
- [8] WANG, Y. Z.; LU, X.; WANG, S. The response of bucket foundation under horizontal dynamic loading. *Ocean Eng* 2006, 33 (7), 964-973.
- [9] Liu, Z.W.; Wang, J.H.; Qin, C.R. Research on the horizontal bearing capacity of bucket foundations. *Chinese Journal of Geotechnical Engineering* 2000, 22(6), 691-695.
- [10] Cai, Z.Y.; Yang, L.G.; Guan Y.F.; Huang, Y.H. Numerical analysis of soil pressure on single bucket wall of new bucket foundation breakwater [J]. *Hydro-Science and Engineering* 2016, 16(5), 39-46.
- [11] Yang, H.D.; Yang, L.G. Computation method of anti-sliding stability of new bucket breakwater [J]. *Port & Waterway Engineering*. 2016, 26(4), 40-44.
- [12] Ding, W.Q.; Zhang, D.; Huang, H.W.; Li, W. Numerical study on the new bucket revetment foundation in the stages of construction and operation. *Journal of Hydraulic Engineering* 2015, 46 (S1), 343-348.
- [13] Cao, Y.Z.; Yao, W.j.; Cheng, Z.K. Analysis of soil pressure and displacement on bucket-based structure under reclamation silt. *Journal of Shanghai University (Natural Science Edition)* 2019, 25(2), 328-336.
- [14] Byrne, B.W.; Houlsy, G.T. Experimental investigations of the cyclic response of suction caissons in sand. *OTC12194*, 2000: 787-795.
- [15] Park, J. S.; Park, D.; Yoo, J. K. Vertical bearing capacity of bucket foundations in sand. *Ocean Eng* 2018, 121(1), 453-456.
- [16] Park, J. S.; Park, D. Vertical bearing capacity of bucket foundation in sand overlying clay. *Ocean Eng* 2017, 134(1), 362-376.
- [17] Wu, F.; Pang, D.G.; Zhang, Z. Fuzzy evaluation for durability of high-pile wharf in service. *Port & Waterway Engineering* 2013, (2), 62-67.
- [18] Li, W.; Cheng, Z.K. Design of bucket-based structure on silt coast. *Port & Waterway Engineering* 2015, 1, 42- 47.
- [19] Liu, H.; Zhang, Q.; Ren, L. Mechanical Performance Monitoring for Prestressed Concrete Piles Used in a Newly-Built High-Piled Wharf in a Harbor with Fiber Bragg Grating Sensor Technology When Pile Driving. *Appl. Sci* 2017, 7 (5), 489.
- [20] Wu, M.; Wang, L.; Xiang, X.H. Research and design of high-pile wharf on weak soil. *Soil Engineering and Foundation* 2009, 23, 26-29.
- [21] CCCC Third Harbor Consultants Co., Ltd. Preliminary design of East Upright-breakwater in of Xuwei Port in Lian Yungang. Shanghai, 2012.
- [22] Sun, D.P.; Yang, Z.L.; Zhu, Q.M. Experimental study on bearing capacity of bucket foundation model of intertidal platform. *Petroleum Engineering Construction* 1999, 2, 12-19.
- [23] Liu, R.; Li B.R.; Ji, J.; Ding, H.Y. Bearing Characteristics of Pile-Bucket Composite Foundation for Offshore Wind Tubine. *Journal of Tianjin University (Science and Technology)* 2015, 48(5), 429-437.
- [24] Wang, Y.; Lu, X.; Wang, S.; Shi, Z. The response of bucket foundation under horizontal dynamic loading. *Ocean Eng* 2006, 33, (7), 964-973.
- [25] Zhang, X.; Gui, J. Study on stability of bucket foundation under backfill. 2018 International Conference on Civil and Hydraulic Engineering, Qingdao, China, 23–25 November, 2018, 2-6.
- [26] Ding, H.; Zhao, X.; Le, C.; Zhang, P.; Min, Q. Towing Motion Characteristics of Composite Bucket Foundation for Offshore Wind Turbines. *Energies* 2019, 12 (19).
- [27] Zhu, C.H. Computation of earth pressure on large diameter cylinder under service ultimate state. *Chinese Journal of Geotechnical Engineering* 2002, 24(3), 313-318.
- [28] Chen, X.; Liu, T.; Jiang, Y.; Liu, H.; Kou, H.; Xu, J.; Liu, X.; Liu, J.; Ma, T.; Feng, T. J. M. G. Stability analysis of suction bucket foundations under wave cyclic loading and scouring. *Mar. Georesour. Geotec* 2018, 36(7), 749-758.
- [29] Liu, M.; Yang, M.; Wang, H. Bearing behavior of wide-shallow bucket foundation for offshore wind turbines in drained silty sand. *Ocean Eng* 2014, 82, 169-179.

- [30] Feng, Y.R.; Wang, Y.B.; Gu, Y.J.; Zhang S.H.; Chu, X.J. Vertical Stability Simulation and Analysis for Single Bucket Foundation Platform. EJGE 2010, 36, 749-758.